CONF-9411236--1

LONG-TERM TESTING*

CONTRACT INFORMATION

Contract Number	ED3201000
Contractor	Oak Ridge National Laboratory P. O. Box 2008 Oak Ridge, TN 37830 Phone: (615) 574-5150 Fax: (615) 574-6098
Contract Project Manager	Mike Karnitz
Principal Investigators	Matt Ferber George A. Graves, Jr.
DOE Project Manager	Gene Hoffman
Period of Performance	October 1, 1993 to October 1, 1994

* Research sponsored by the DOE, Assistant Secretary for Energy Efficiency and Renewable Energy, Office of Industrial Technologies, Industrial Energy Efficiency Division and Advanced Turbine Systems Program, under Control DE-AC05-84OR21400 With Martin Marietta Energy Systems.

DISCLAIMER

Portions of this document may be illegible in electronic image products. Images are produced from the best available original document.

OBJECTIVES

The primary goal of this research is to determine the long-term survivability of ceramic materials for industrial gas turbine applications. Research activities in this program focus on the evaluation of the static tensile creep and stress rupture (SR) behavior of three commercially available structural ceramics which have been identified by the gas turbine manufacturers as leading candidates for use in industrial gas turbines. Tensile creep data will be generated in air by measuring creep strain as a function of time, applied stress, and temperature. The SR resistance will be evaluated by continuing each creep test until the specimen fails. For each material investigated, a minimum of three temperatures and four stresses will be used to establish the stress and temperature sensitivities of the creep and SR behavior. The test matrix utilized in this program is intended to extend the test conditions investigated by the engine component manufacturers. In the latter case, these conditions focus primarily upon the evaluation of the creep and SR behavior of two candidate materials at one temperature only. Consequently, the temperatures chosen for the current effort will bracket that used by the engine component manufacturers. Because existing data for many candidate structural ceramics are limited to testing times less than 2,000 h, this program will focus on extending these data to times on the order of 10,000 h, which represents the lower limit of operating time anticipated for ceramic blades and vanes in gas turbine engines.

A secondary goal of the program will be to investigate the possibility of enhancing life prediction estimates by combining interrupted tensile SR tests and tensile dynamic fatigue tests in which tensile strength is measured as a function of stressing rate. The third goal of this program will be to investigate the effects of water vapor upon the SR behavior of the three structural ceramics chosen for the static tensile studies by measuring the flexural strength as a function of stressing rate at three temperatures.

BACKGROUND INFORMATION

DOE-OIT (Office of Industrial Technology) has initiated a program to develop ceramic components for use in industrial gas turbines. The objective of this program is to improve the efficiency of land-based gas turbines that are used for industrial cogeneration. As part of this program, Battelle Columbus completed an assessment and developed a program plan in March 1991. The assessment reviewed the status of ceramic materials in the context of gas turbine engine development and concluded that significant performance gains could be expected from the use of ceramics. Based on the assessment and manufacturers recommendations, a five-year program plan was developed. The program was designed to bring ceramic technology to the point where short-term reliability and engine performance had been demonstrated. This would provide a technology base from which manufacturers' could move forward with engine performance improvements, field testing, and commercial development.

Based on the program plan, OIT issued a solicitation and selected Solar Turbines Incorporated for the development of ceramic gas turbine components. Solar Turbines started working in late FY 1992. One of the critical areas outlined in their program was a long-term materials testing program. Land-based gas turbines are significantly different from automotive gas turbines in that they are designed to operate for 50,000 h or greater (compared to 5,000–10,000 h). Long-term materials tests are needed to determine the survivability of the materials for land-based applications. This paper outlines the long-term testing conducted at Oak Ridge National

Laboratory (ORNL) and University of Dayton Research Institute (UDRI) in support of the new program with Solar Turbines.

PROJECT DESCRIPTION

For long-term testing, ORNL will work with Solar Turbines in identifying materials to be tested. A minimum of three materials will be chosen for evaluation. For each material identified, tensile creep data will be generated in air by measuring creep strain as a function of time, applied stress, and temperature. The SR behavior will be evaluated by continuing each creep test until specimen failure occurs. A minimum of three temperatures and four stresses will be used to establish the stress and temperature sensitivities of the creep and SR behaviors. The temperatures chosen for the ORNL effort will bracket that used by the engine component manufacturers in their "in-house" creep and SR testing effort.

For each temperature considered, the creep and SR behavior will be established using a minimum number of 26 tensile specimens. Five additional specimens will be used to measure the fast fracture strength. The ORNL button-head specimen configuration will be used for these measurements. In order to establish long-term mechanical survivability, the applied stresses will be adjusted to obtain failure times ranging from 10–100, 100–1,000, 1,000–5,000, and 5,000–10,000 h. Initial estimates of these stresses will be based on preliminary mechanical reliability diagrams constructed from flexural dynamic fatigue and fracture toughness data generated at each temperature. Specimens not failing within the allotted time range will be fractured at temperature to determine the residual strength.

For each material investigated, the associated creep and SR data will be used to generate a mechanical reliability diagram describing the time-to-failure and failure mode (creep damage versus slow crack growth) as functions of stress and temperature. The applicability of various creep and SR models (Monkman-Grant, Sherby-Dorn, Larson-Miller, etc.) to the description of the experimental data will also be investigated. The final material selection will be based upon a comparison of these diagrams.

A secondary goal of the program will be to investigate the possibility of enhancing life prediction estimates by combining interrupted tensile SR tests and tensile dynamic fatigue tests in which tensile strength is measured as a function of stressing rate. This technique will be applied to one material at one temperature for interrupted times of 100 and 1,000 h. The data will be used to generate SR curves which will then be compared with actual results.

The third goal of this program will be to investigate the effects of water vapor upon the SR behavior of the three structural ceramics chosen for the static tensile studies by measuring the flexural strength as a function of stressing rate at three temperatures. If water vapor in the environment is found to be a problem, additional tensile creep and SR measurements will be made for verification purposes.

This work will be composed of the following eight Tasks:

Task 1 - Development of an experimental test plan, which outlines the scope of the test matrix.

Task 2 - Creep/SR comparison study between UDRI and ORNL.

Task 3 - Design, procurement, and initiation of tensile test facilities required for the 10,000 hour tests.

Task 4 - Procurement of the flexure and tensile specimens.

Task 5 - Long-term mechanical testing of three candidate materials. Initially, this effort will include the utilization of flexural dynamic fatigue to more clearly define the stress levels for the subsequent tensile creep/SR tests.

Task 6 - Develop and initiate experimental test plan for combining interrupted SR and dynamic fatigue.

Task 7 - Perform flexural dynamic fatigue studies to address the effects of water behavior on SR behavior.

Task 8 - Prepare final report.

RESULTS

Comparison Study

A study comparing the creep and SR measurement capabilities of ORNL and UDRI was continued during this reporting period. Because UDRI will assist ORNL in the completion of the long-term test matrix, any discrepancies in experimental data arising from the test equipment and methodologies used by the two laboratories must be identified and corrected early in the program. The comparison study involves the evaluation of the creep and SR behavior of a hot isostatically pressed (HIPed) silicon nitride (NT154 and NT164)[a] at 1370°C, a dense silicon carbide (SA SiC)[b] at 1500°C, and an aluminum oxide (AD99)[c] at 1150°C. Figure 1 compares strain versus time data generated for the NT154 at a stress of 150 MPa. The agreement between UDRI and ORNL is excellent. The difference between respective failure times is well within statistical scatter reported for this material.[1] As shown in Fig. 2, which is a plot of strain versus time for SA SiC, agreement between the UDRI and ORNL results was reasonably good. The differences between respective curves are well within statistical scatter reported for this class of high temperature materials.[1] Based on the comparisons conducted to date, there appears to be no discrepancy in creep strain measurement techniques.

Creep/Stress Rupture Facility

During this reporting period, considerable emphasis was placed upon the specification, procurement, and installation of the eight mechanical test machines required for the long-term testing phase of the program. Although these machines will be primarily used for static stress measurements (e.g., creep and stress rupture), they will also be capable of load-to-failure tests over a wide range of loading rates. Figure 3 illustrates the major components of the creep/stress rupture test machine. The load frame is similar to that used for stress relaxation tests. An electro-mechanical actuator attached to the outer position of a 20-to-1 lever arm provides for application of the mechanical loads. The load train includes the grips for the ORNL button-head tensile specimen (Fig. 4) and special knife-edge couplers which may be adjusted to minimize bending in the tensile specimen. A load cell provides the necessary feed-back signal to the electronics used to control the electromechanical actuator. A short two-zone resistance furnace located between the water-

---

[a] NT154 and NT164 silicon nitride ceramics, Saint-Gobain/Norton Industrial Ceramics Corporation, Northboro, MA.

[b] Sintered Alpha silicon carbide, Carborundum Company, Niagara Falls, NY.

[c] AD99 aluminum oxide, Coors Company, Golden, CO.

cooled grips provides for testing at temperatures up to 1500°C. The specimen displacements are measured over a 25.4 mm gage length using a direct contact capcitance extensometer.

When conducting a test, the load is maintained at the desired level by inputting the proper setpoint voltage to the controller where 0 to 10V corresponds to 0 to full-scale load. A second 0 to 10 V signal is used to set the actuator speed. This arrangement allows one to conduct either constant load tests or load-to-failure tests as a function of load rate. Both of the control signals are supplied by a data acquisition system (DAS) and personal computer. The DAS also accepts input signals from the load cell, extensometer, and temperature controller.

The operational tests performed at the seller's plant, Applied Test Systems (ATS), included (1) measurement of the percent bending as a function stress, (2) measurement of the temperature gradients across the gage section of the button-head specimen, and (3) verification of the load controller operation. The percent bending was measured using a PY6 silicon nitride[d] button-head specimen having eight strain gages in the gage section (Fig. 4). The four gages located at the specimen midspan were used to measure the angular misalignment.[2,3] The magnitude of the concentric misalignment or "S" bending[2,3] was determined from the gages located at the ends of the gage section. A sophisticated strain gage conditioning system with a programmable "front-end processor" was used to simultaneously condition the strain gage signals, calculate the percent bending strain, and record the strain, percent bending error, and the applied load (stress).

Applied Test Systems personnel also demonstrated the use of a newly developed SLVC alignment fixture for the real-time measurement of bending across opposing shanks of the tensile specimen. This device, which was mechanically clamped to the specimen shanks, basically gave an over-all indication of the longitudinal strain at 90° intervals over the entire gage section. In this sense, it served the same purpose as the four strain gages located at the specimen midspan. The readings from the alignment device were used to minimize bending via adjustments to the knife-edge coupler.

Three separate bending measurement tests, designated as Trials 1 through 3, were conducted. For Trial 1, no adjustments were made to the knife-edge grips. The percent bending decreased as the stress increased. At an applied stress of 150 MPa, the percent bending values for axial and concentric misalignments were 9.2 and 8.1, respectively. These numbers were subsequently reduced to 2.4 and 0.8 by adjusting the knife-edge grips in accordance with the strain readings supplied by the alignment device.

In order to examine the ruggedness of the alignment procedure, the specimen was unloaded and then subjected to two load/unload cycles during which time the percent bending was measured (Trial 2). The percent bending values for axial and concentric misalignments measured at 150 MPa were 4.8 and 2.7, respectively during the first cycle and 4.7 and 2.7, respectively during the second cycle. As a final verification, the specimen was completely unloaded before initiating another test. The percent bending measured at a given stress during Trial 3 was comparable to that measured in Trial 2. The fact that these percent bending versus applied stress curves were not strongly influenced by load/unload cycles indicates that the alignment process was fairly robust. More importantly, the use of the strain readings from the SLVC alignment device to minimize the percent bending (as measured by the strain gages) was found to be a valid approach.

In the next evaluation test, a silicon nitride button-head specimen having three equally spaced Type S thermocouples attached to the gage section was used to measure temperature gradients. Although it was possible to independently control the top and bottom zones on the furnace (through the specification of separate setpoints), no attempt

---

[d] PY6 silicon nitride, GTE Laboratories, Inc., Waltham, Massachusetts.

was made to minimize the temperature gradients. For temperatures above 1000°C, the center and top regions were within 5°C of one another while the bottom region of the gage section was always 10 to 18°C hotter. Preliminary adjustments of the bottom zone controller indicated that the temperature difference between the bottom and center points on the specimen could be reduced to less than 5°C. For temperatures below 1000°C, the temperatures along the top and bottom regions were comparable while the specimen midpoint was 5 to 8°C cooler. This effect was attributed to the presence of an insulating spacer between the top and bottom zones of the furnace. The purpose of this spacer is to eliminate hot spots along the specimen midspan arising from radiation which becomes an important factor only at the higher temperatures (>1000°C). Therefore at temperatures below 1000°C, it should be possible to reduce the temperature gradients between the center and outer regions in the gage section by removing this spacer.

The verification tests of the load controller involved inputting a fixed control signal (0 to 10 V) and then observing the response of the load system, which included a metallic specimen. In general, the load on the specimen was held to within 10 N of the specified setpoint. The minimum and maximum loading rates were also found to be acceptable.

Following delivery of the eight SR/creep machines to ORNL, additional verification tests were conducted including (1) measurement of the percent bending as a function of stress, (2) assessment of the load control capabilities, (3) verification of the computer interface and software, and (4) measurement of extensometer resolution, hysteresis, and linearity.

The percent bending was measured using the same setup described above. Three separate bending measurement tests, designated as Trials 1 through 3, were conducted. In Trial 1, the PY6 was loaded to 7 kN and the grips adjusted to minimize bending. The adjustment was based on the output from the SLVC alignment fixture, which was mechanically clamped to the specimen shanks. The specimen was unloaded to 1 kN and reloaded to 7 kN. As shown in Fig. 5, this load cycling did not significantly affect the axial or concentric bending numbers both of which remained below the target value of 5%. In Trial 2, the specimen was unloaded to 1 kN and the alignment fixture removed. The specimen was then reloaded to 7 kN. The bending numbers still remained below the 5% target indicating that removal of the alignment fixture had minimal influence on the specimen alignment. In Trial 3, the effect of introducing the contact extensometer upon specimen bending was examined. Even with a 3.0 psi side pressure exerted with the extensometer, the specimen bending (at 7 kN) was at or below the 5% level.

In assessment of the load control capabilities, the setpoint of the load controller was abruptly changed and the load response measured. Little or no over-shoot (under-shoot in the case where the load was abruptly decreased) occurred as the load approached its setpoint.

The verification tests of the computer interface involved confirming that all signals supplied by the test machine were properly received by the data acquisition system. The operation of the data acquisition software, which was developed using a commercial package (LabVIEW® 2[e]), was also examined. Initial problems with the stability of the temperature signals was traced to a ungrounded temperature controller in the electronics console. The load signal was found to have an acceptable signal-to-noise ratio as long as the lever arm drive motor was disabled. However, excessive noise was introduced into the load signal when the drive motor was activated. The introduction of analog filters was found to reduce this noise to an acceptable level.

Operational tests with the software were also completed. The LabVIEW® 2 environment allows for the creation of virtual instrument control panels on the computer screen (Fig. 6). For each frame,

---

[e] LabVIEW® 2 software manufactured by National Instruments, Austin, TX.

load, extensometer displacement, and the upper and lower furnace zone temperatures are continuously displayed. Digital indicators include local/remote status, specimen break, furnace/water flow interlocks, and electrical supply status (L/R STAT, BREAK, SAFETIES, AND MAINS in Fig. 6). Provisions for digital control of the drive motor and furnace output relay are also available. When the test frame is in the remote mode, the load and actuator speed are controlled by the Setpoint and Speed settings in Fig. 6.

The acceptance tests for the ATS extensometer were less successful. As shown in Fig. 7, extensometer hysteresis was found to be a major concern. Data generated with a second capacitance contact extensometer[f] is included in this figure for purposes of comparison. The hysteresis problem is believed to be a result of relative movement of the pivot points associated with the support design of the extensometer rods. Because of these results, the ATS extensometers were rejected and a new order placed for eight capacitance contact extensometers manufactured by the alternate vendor. Verification tests conducted on these new extensometers showed that their performance was within the required specifications.

As-Received Materials and Inspection

The matrix of test specimens for each of the three ceramic materials being examined in this program is given in Table 1. The fabrication of the NT164 is through pressure slip casting for the green state and hot isostatic pressing (HIPing) for the final densification. The microstructure typically consists of β silicon nitride grains having a grain width of less than one micron and an aspect ratio range of 4 to 8. Depending upon processing, the α silicon nitride content can range from 5 to 40%. The SA SiC is a sintered silicon carbide which is fabricated in the green-state by injection molding. Additions of small amounts of carbon and boron are used to assist the densification during the sintering step. Post-sinter HIPing is also used to improve density and reduce defect size. The microstructure of this material typically consists of a silicon carbide grains ranging size from 2 to 8 μm. Finally, the SN88 silicon nitride is injection molded followed by gas pressure sintering.

All tensile specimens were dimensionally inspected using a commercial coordinate measuring machine (CMM).[g] The inspection protocol (Fig. 8) included measurement of the shank diameters, gage diameters, button-to-shank radii, and the coaxiality between the shank and gage regions. The typical measuring time per specimen was 25 minutes which is considerably less than that required for manual inspection with an optical comparator. A comparison of the coaxiality measurements is given in Figs. 9 through 11 for the NT164, SN88, and SA SiC, respectively. The maximum allowable coaxiality of 5.0 μm (designated by the bold horizontal line) was based on the requirement that the contribution to bending arising from the specimen itself be negligible (bending < 1%). Clearly, most of the SN88 specimens exceeded the specified value while the majority of the SA SiC and NT164 specimens were below the 5.0 μm limit. It should be noted that a coaxiality of 30 μm will introduce 3 to 4% of bending from the specimen alone. In general, most of the SA SiC and NT164 specimens satisfied the required dimensional tolerances while fairly significant deviations from the specified tolerances were measured for the SN88 specimens.

Stress Relaxation Testing

Studies to examine the effect of stress

[f] Manufactured by Instron Corporation, Canton, MA.

[g] LEITZ Coordinate Measuring Machine, distributed by Brown & Sharpe, North Manufacturing Company, Kingstown, RI. 02852.

relaxation upon creep behavior were also initiated this reporting period. Motivation behind the stress relaxation testing is twofold: (1) to investigate the validity of using this technique for accelerating the generation of creep rate-stress data, and (2) to generate data that may be readily used to predict stress relaxation in industrial gas turbine components that are subjected to constant displacement or strain during service. Stress relaxation and its affect upon long-term mechanical survivability is an important consideration in components which are constrained in movement. In the actual experiment, the strain applied to a button-head tensile specimen is increased to a specified value under load control. The test machine is then transferred to strain control to maintain a constant strain, and the relaxation of stress was monitored as a function of time. A stable extensometer signal is crucial in order that a valid stress relaxation test results. The testing apparatus necessary to perform stress relaxation requires that an extensometer signal comprises a portion of electronic, closed-loop control of the testing machine. Due to the high stiffness of these structural ceramics, a stable signal from the high temperature extensometer is imperative; otherwise wide stress fluctuations will result during the relaxation process. A Lexan box surrounds the extensometer and shields its circuitry. A stable flow of air is maintained within the Lexan box during the stress relaxation test and this further stabilizes the temperature of the circuitry. These provisions result in typical strain fluctuations of ± 0.1 μm. As an example, this fluctuation will manifest itself into a stress fluctuation of $\pm \approx 1.5$ MPa for a material with a Young's Modulus of 300 GPa and a button-head diameter of 6.35 mm.

For these test conditions, the total strain (ε_{tot}) may be represented as the sum of the elastic (ε_{el}) and plastic (creep) strain (ε_{pl}), or

$$\varepsilon_{tot} = \varepsilon_{el} + \varepsilon_{pl}. \qquad (1)$$

Taking the time derivative and recognizing that for fixed strain, $d\varepsilon_{tot}/dt = 0$, one has

$$d\varepsilon_{el}/dt = - d\varepsilon_{pl}/dt. \qquad (2)$$

Because the elastic strain rate is equal to $(d\sigma/dt)/E$, where $d\sigma/dt$ is the instantaneous stressing rate and E is Young's Modulus, the plastic strain rate is given by

$$d\varepsilon_{pl}/dt = - (d\sigma/dt)/E. \qquad (3)$$

Using these expressions, one may determine the creep rate as a function of stress over many orders of magnitude. The advantage of a stress relaxation test is that several decades of creep rates are measured in several hours of experimentation with one specimen; whereas equivalent generated data using static creep tests require numerous specimens (one stress-strain rate data point per specimen) tested over a range of applied stresses.

Figure 12 shows a typical stress relaxation curve generated at 1370°C with NCX-5102[h] silicon nitride. Figure 13 compares the $d\varepsilon_{pl}/dt$ versus stress curve determined from the stress relaxation data with corresponding curves obtained from static stress tests at 125 and 140 MPa. The creep rates from the static stress tests were determined at specimen failure (minimum strain rate), at test commencement (maximum strain rate), and when a total of 2810 με had accumulated. The motivation for including the static creep rates measured at an accumulated strain of 2810 με is that the data from the relaxation test were also generated when the specimen had accumulated 2810 με. As shown in Fig. 13, the data generated from the stress relaxation test is situated in the range between the minimum and maximum strain rates. Further exploratory studies of this technique and its applicability are under investigation.

---

[h] NCX-5102 silicon nitride ceramics are manufactured by St. Gobain-Norton Industrial Ceramics Corp., Northboro, MA

Stress relaxation testing of two SN88 (NGK) silicon nitride and two SN253 (Kyocera) specimens was also completed during this reporting period. For each material, one specimen was loaded to an initial stress of 276 MPa (40 ksi) and the other was loaded to 414 MPa (60 ksi); both were tested at 1300°C (2372°F). As a supplement, the stress relaxation behavior of NCX-5102 silicon nitride specimens were also examined at the same test conditions. For both stresses, the rate of stress relaxation increased in the order (NCX-5102<SN253<SN88). Although all three silicon nitrides exhibited viscoelastic behavior, it is speculated that the more extensive relaxation of the SN88 may be due to a greater volume fraction and/or less refractoriness of the grain boundary phase. In terms of the creep rate versus stress curves generated from the stress relaxation data, the creep exponents increased in the following order: NCX-5102 > SN253 > SN88. Furthermore, for a fixed stress, the creep rate was largest for the SN88 and smallest for the NCX-5102.

Creep/Stress Rupture Testing

Creep/stress rupture testing of the SN88 tensile specimens was initiated at 1350, 1150, and 1038°C during the present reporting period. The choice of applied stresses was based upon the fast fracture strengths measured at each of three temperatures. Preliminary results from the first test at 1350°C are shown in Fig. 14. Due to unexpectedly rapid creep deformation, the extensometer range was exceeded prior to specimen failure. This extensive creep is consistent with the measured stress relaxation behavior described above. Microstructural analysis of this specimen is underway.

FUTURE WORK

Future efforts will focus upon the completion of the SR/creep measurements of the three materials listed in Table 1. Microstructural analysis and x-ray diffraction will be used to study changes in the microstructure and intergranular phase composition arising from the long-term testing. The effect of water vapor upon the time-dependent mechanical behavior will also be investigated. Finally, methods for combining interrupted tensile SR tests and tensile dynamic fatigue tests, in which tensile strength is measured as a function of stressing rate, will be studied in an effort to enhance life prediction estimates.

REFERENCES

(1) M. N. Menon, H. T. Fang, D. C. Wu, M. G. Jenkins, and M. K. Ferber, "Creep and Stress Rupture Behavior of an Advanced Silicon Nitride," submitted to the Journal of the American Ceramic Society for publication.

(2) A. Rudnick, C. W. Marschall, W. H. Duckworth, B. R. Emrich,*The Evaluation and Interpretation of Mechanical Properties of Brittle Materials*. AFML-TR-67-316, Air Force Materials Laboratory, Wright Patterson Air Force Base, Ohio, 1968.

(3) C. G. Larsen, L. E. Johnson, and L. G. Mosiman, "Gripping Techniques and Concerns for Mechanical Testing of Ultra-High Temperature Materials," MTS Systems Corporation Technical Publication (1993).

Table 1. Summary of Tensile and Flexure Specimen Matrix Required for the Program

Material	Supplier	No. of Tensile Specimens	No. of Flexure Specimens
SA SiC	Carborundum Company Niagara Falls, NY 14302-0832	50	205
NT164 Si_3N_4	Saint-Gobain/Norton Industrial Ceramics Northboro, MA 01532-1545	126	205
SN88 Si_3N_4	NGK Insulators, LTD Nagoya, Japan	50	205

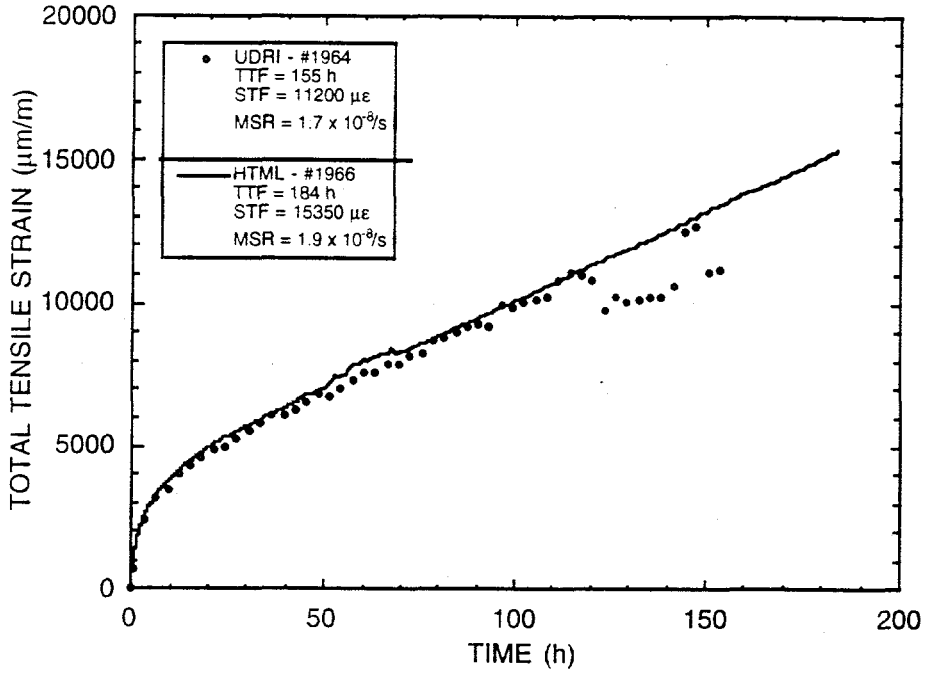

Figure 1. Comparison of Strain Versus Time Data Generated for the NT154 at a Stress of 150 MPa

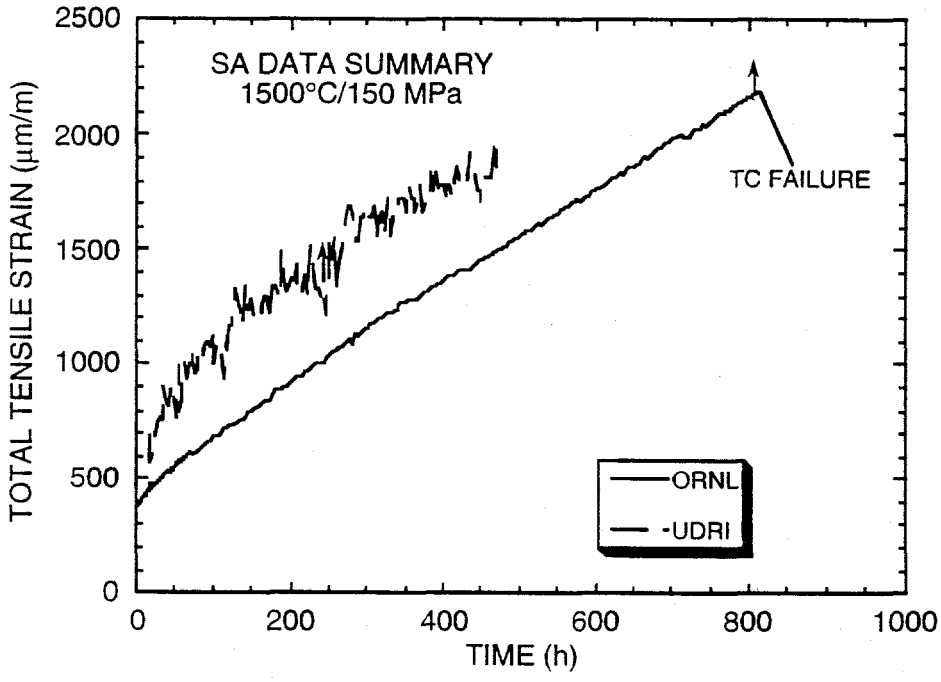

Figure 2. Comparison of Strain-Time Curves Generated for SA SiC at UDRI and ORNL

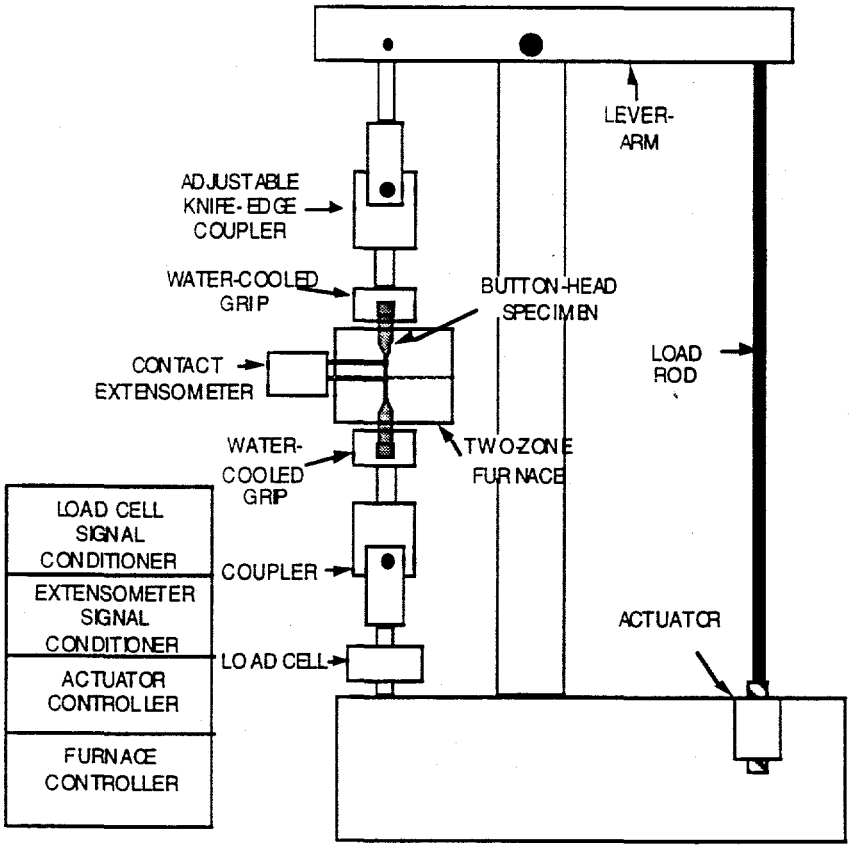

Figure 3. Major Components of the Creep/Stress Rupture Test Machine

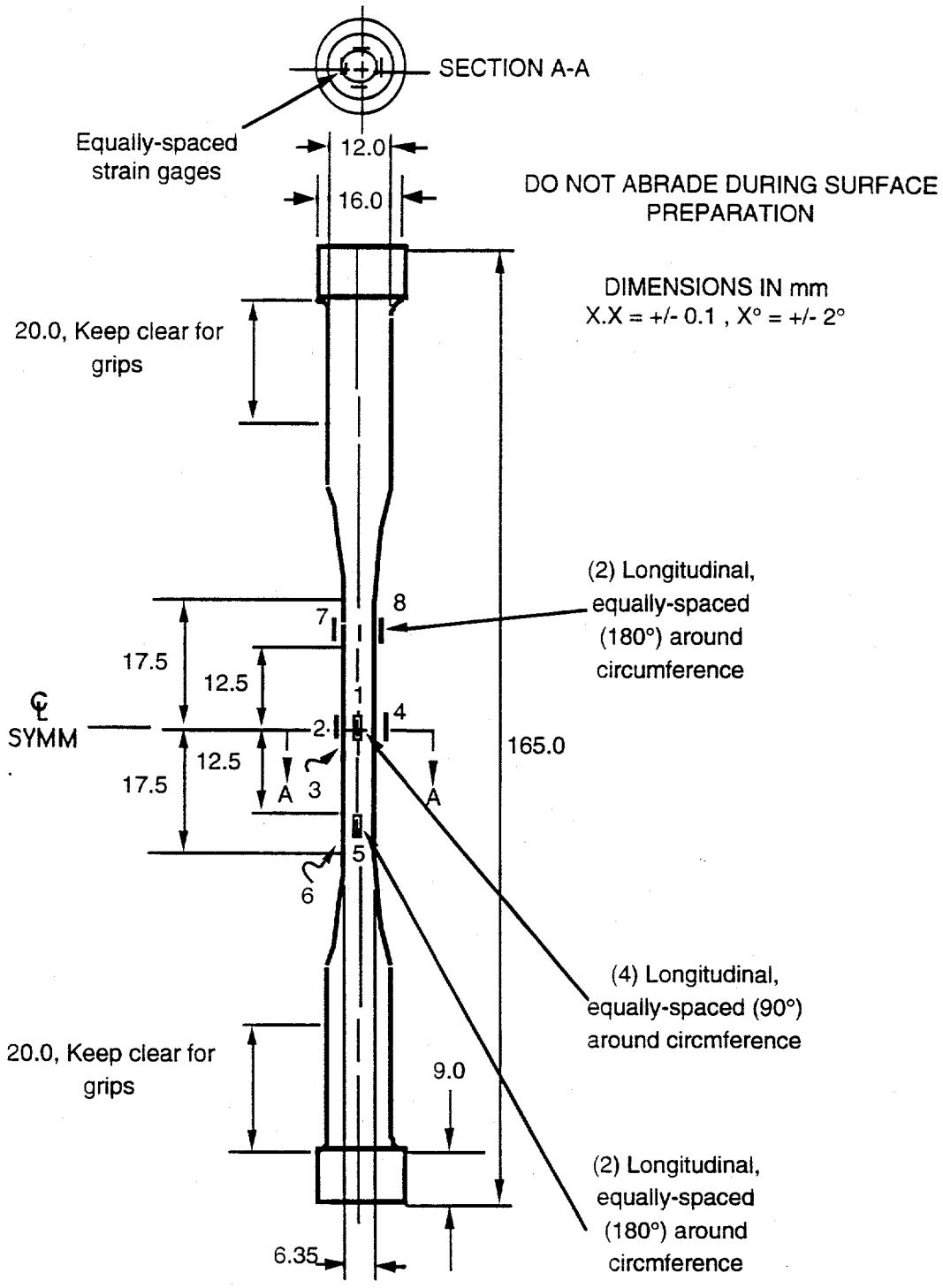

Figure 4. Strain gage Specimen Used to Measure Bending

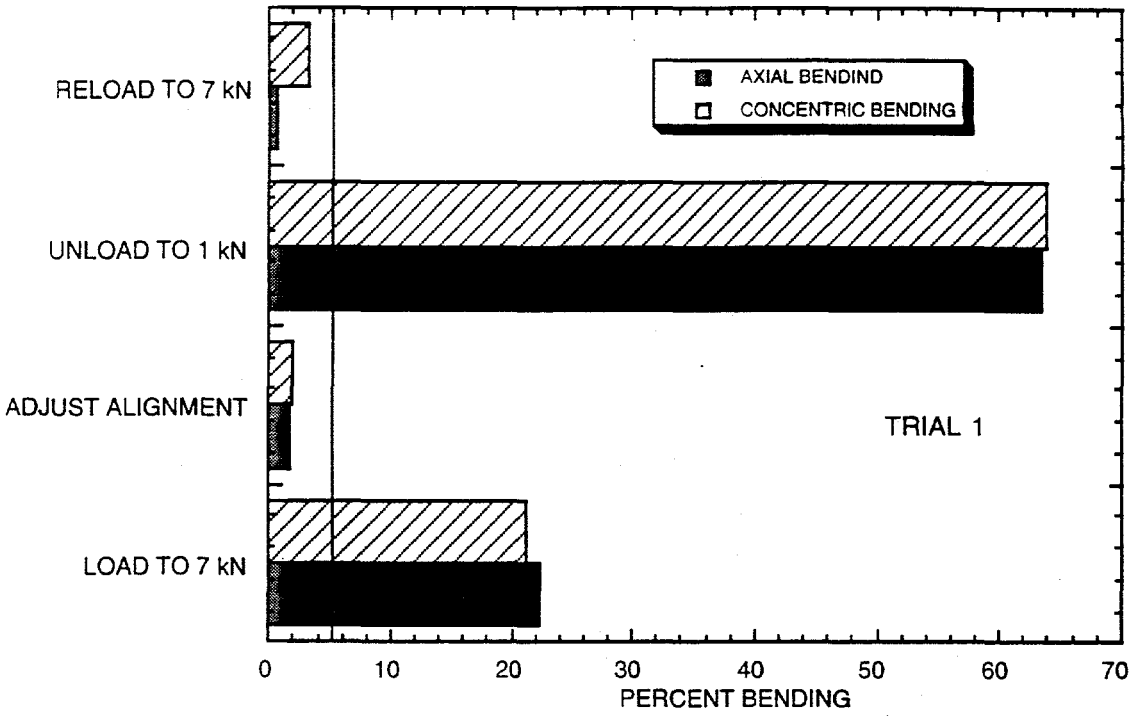

Figure 5. Summary of Percent Bending Values Obtained in Trial 1 Tests

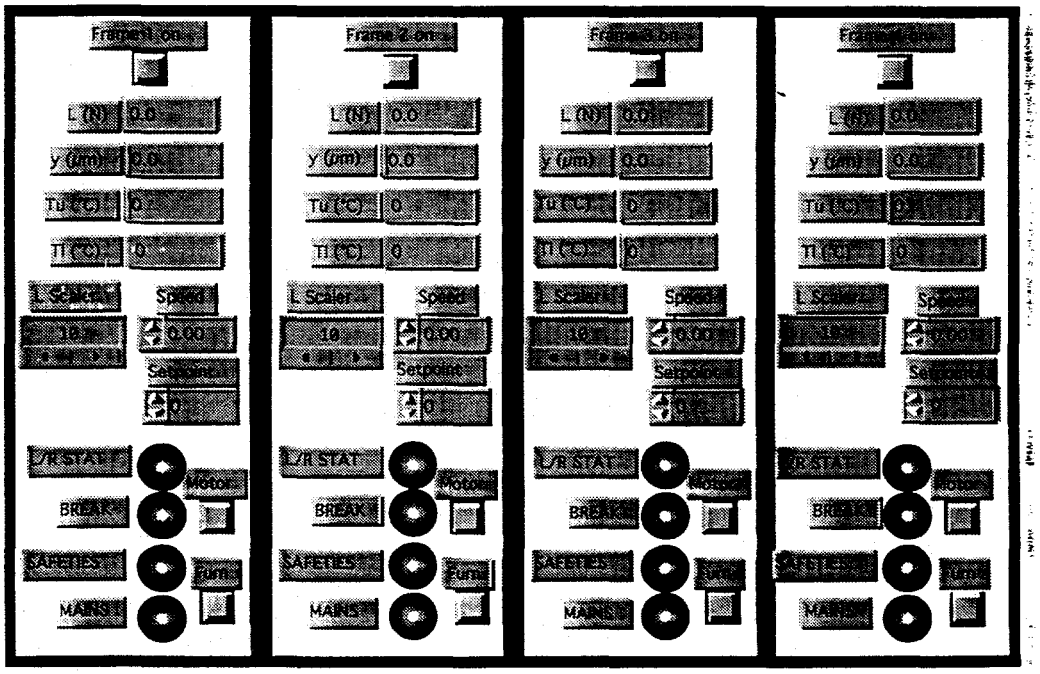

Figure 6. Virtual Instrument Control Panel used for Data Acquisition and Control

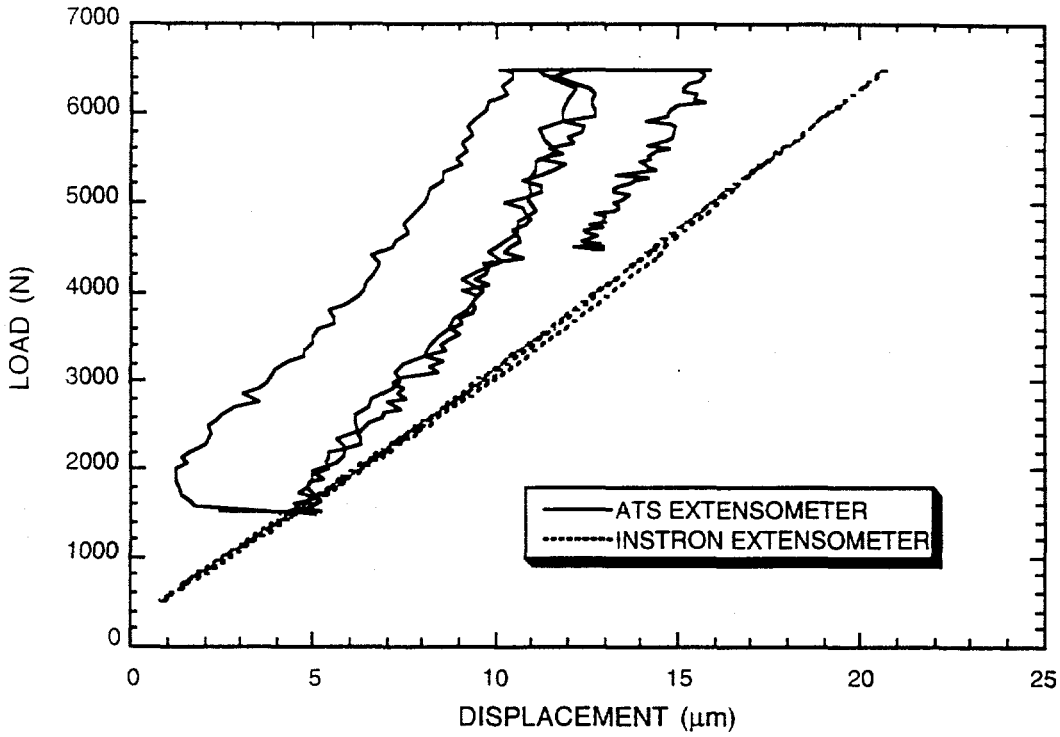

Figure 7. Comparison of Load-Displacement Curves Obtained with ATS and Instron Extensometers

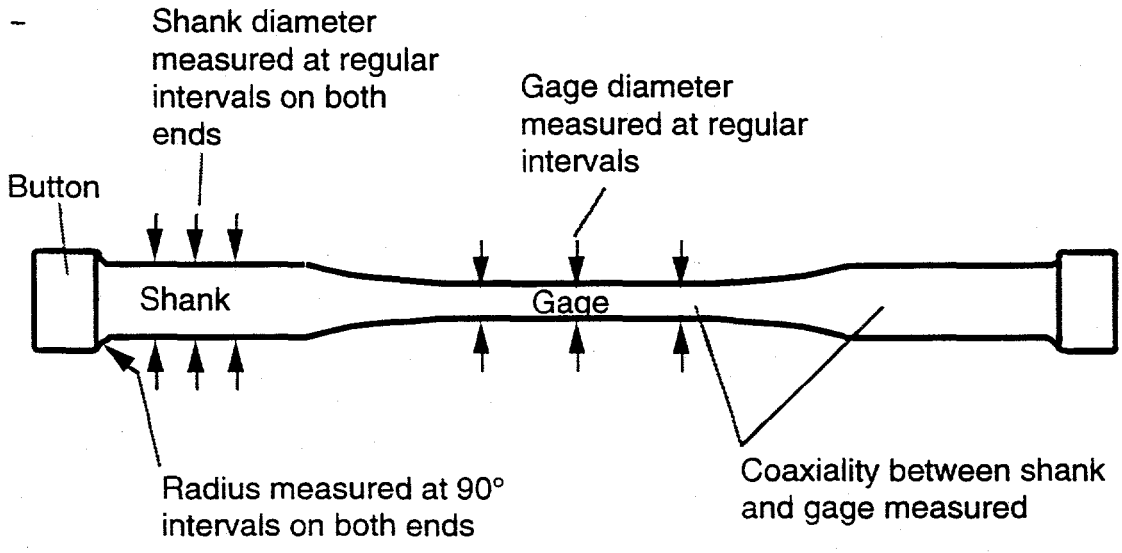

Figure 8. Schematic Representation of Inspection Protocol used for Ceramic Button-Head Tensile Specimens.

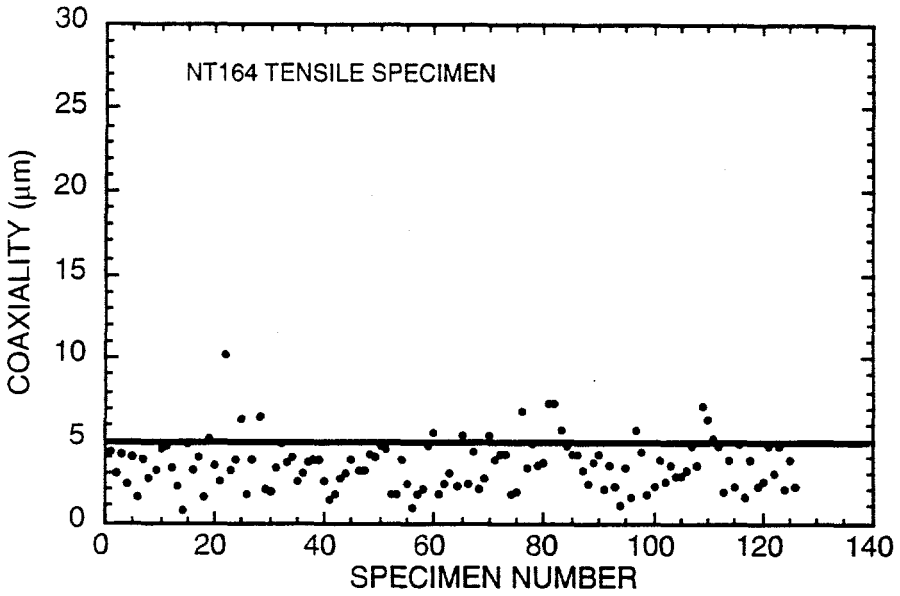

Figure 9. Summary of Coaxiality Measurements for the NT164 Silicon Nitride Button-Head Specimens

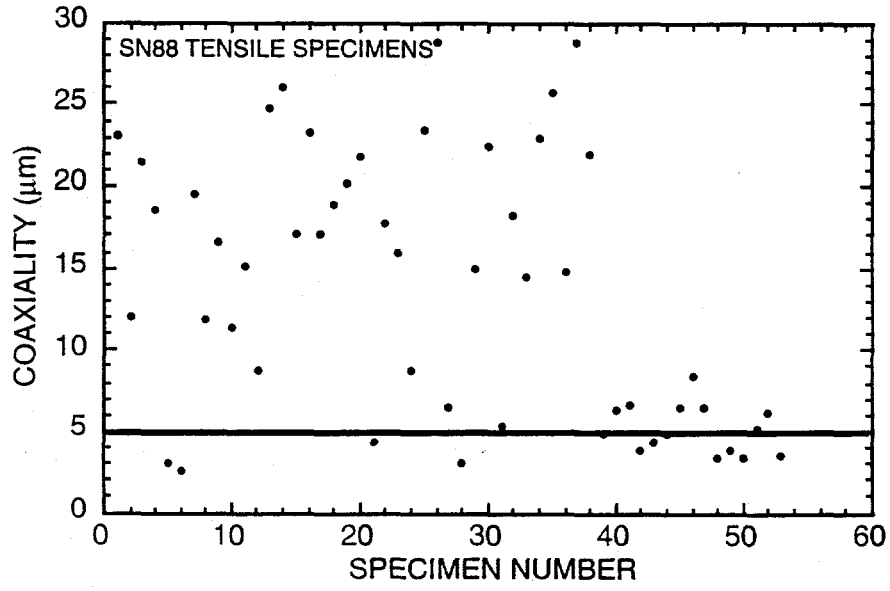

Figure 10. Summary of Coaxiality Measurements for the SN88 Silicon Nitride Button-Head Specimens.

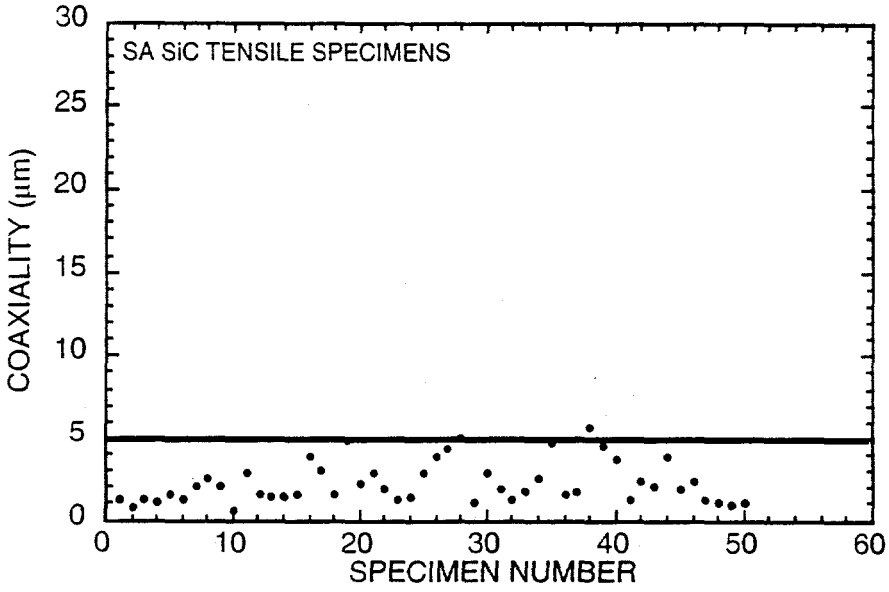

Figure 11. Summary of Coaxiality Measurements for the SA Silicon Carbide Button-Head Specimens

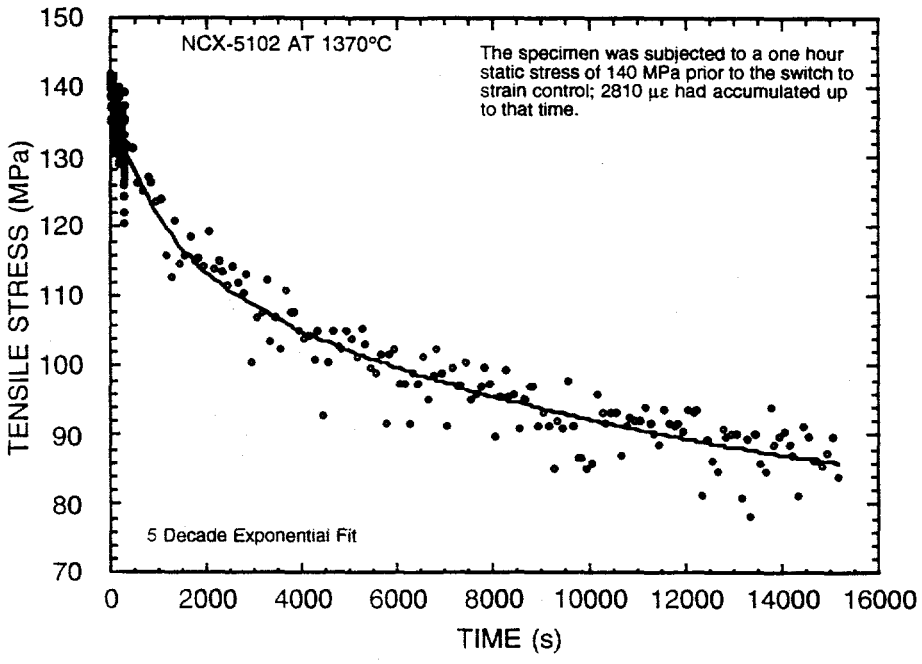

Figure 12. Typical Stress Relaxation Curve Generated at 1370°C with NCX-5102 Silicon Nitride

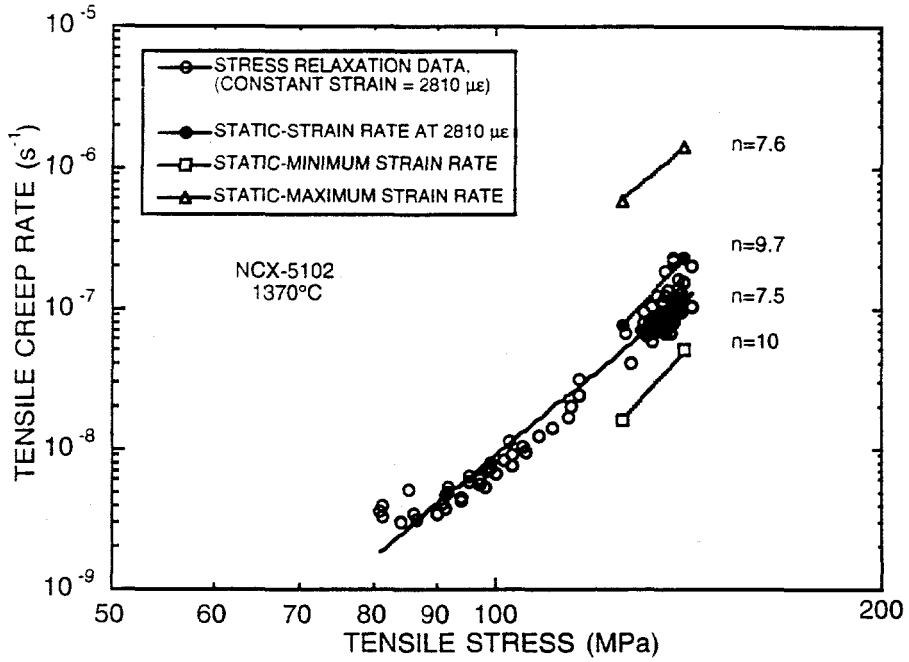

Figure 13. Comparison of the $d\varepsilon_{pl}/dt$ Versus Stress Curve Determined from the Stress Relaxation Data with Corresponding Curves Obtained from Static Stress Tests at 125 and 140 MPa

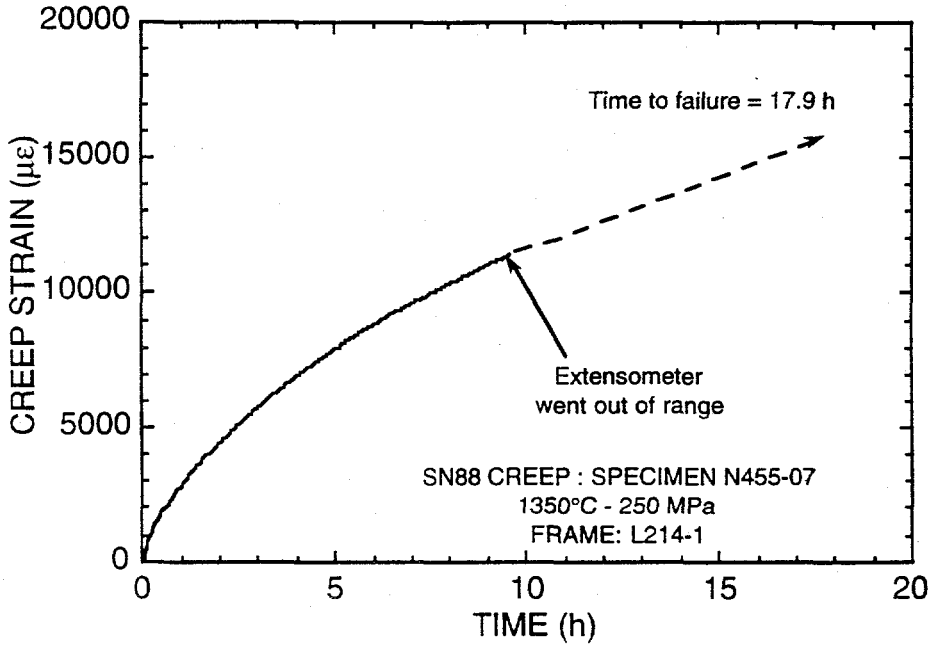

Figure 14. Time-Dependence of Tensile Creep Strain Measured for SN88 Silicon Nitride at 1350°C and 250 MPa.